International Journal of Bifurcation and Chaos, Vol. 7, No. 6 (1997) 1367–1374

SIMULATING QUADRATICALLY NONLINEAR RANDOM PROCESSES

BARRY VANHOFF and STEVE ELGAR
School of Electrical Engineering and Computer Science,
Washington State University, Pullman, WA 99164-2752, USA

Received November 22, 1996; Revised June 10, 1997

A technique to generate realizations of quadratically nonlinear non-Gaussian time series with a desired ("target") power spectrum and bispectrum is presented. Specifically, by generating a Gaussian time series (using amplitude information from the target power spectrum and random phases) and passing it through a quadratic filter (that uses phase information from the target bispectrum), a realization of a quadratically nonlinear random process with a specified power spectrum and bispectrum can be produced. Second- and third-order statistics from many realizations of simulated nonlinear time series compare well to those from the original time series providing the target power spectrum and bispectrum, with deviations consistent with theory. The simulation technique is shown to simulate accurately ocean waves in shallow water, which are well known to be quadratically nonlinear.

1. Introduction

Realizations of time series with a specified power spectrum and Gaussian statistics can be generated by coupling random phases with Fourier amplitudes determined from the spectrum. The simulated linear time series can be used to test for nonlinearities in observations [Theiler *et al.*, 1992]. Nonlinear and non-Gaussian random processes cannot be represented by a linear combination of independent Fourier components with random phases. For example, quadratic nonlinearities result in phase coupling between triads of Fourier components, with the corresponding nonrandom phase relationships given by the bispectrum [Hasselmann *et al.*, 1963; Nikias & Raghuveer, 1987; Elgar & Chandran, 1993]. Time series for quadratically nonlinear deterministic processes can be reconstructed from the bispectrum [Matsuoka & Ulrych, 1984; Nikias & Raghuveer, 1987; Alshebeili & Cetin, 1990; Dianat & Raghuveer, 1990]. Quadratic time-invariant filters driven by white Gaussian noise have also been used to model bispectra [Bondon *et al.*, 1993; Bondon & Krob, 1995]. In the present study, a methodology to generate realizations of quadratically nonlinear random processes with a specified ("target") power spectrum and bispectrum is developed.

A brief review of techniques to simulate realizations of a Gaussian process is presented in Sec. 2, followed by a description of a new methodology to generate realizations of a quadratically phase coupled non-Gaussian random process (Sec. 3). In Sec. 4 the new technique is used to produce simulations of shallow water ocean surface gravity waves (well known to be quadratically nonlinear [Freilich & Guza, 1984]) with target power spectra and bispectra determined from observations. Conclusions follow in Sec. 5.

E-mail: bvanhof@eecs.wsu.edu
E-mail: elgar@eecs.wsu.edu

2. Simulation of a Gaussian Process

A finite-length time series $x(n)$ can be represented as [Rice, 1944, 1945]

$$x(n) = \sum_{k=1}^{K} a_k \cos(2\pi f_k n) + b_k \sin(2\pi f_k n) \qquad (1)$$

where a_k and b_k are Gaussian distributed random variables with zero mean and variance $P(f_k)$, the power of $x(n)$ at frequency f_k, defined by

$$P(f_k) = E[X(f_k)X^*(f_k)] = E[|X(f_k)|^2]\,. \qquad (2)$$

The $X(f_k) = X^*(-f_k)$ are the Fourier coefficients of $x(n)$, $f_k = kf_N/K$ where f_N is the Nyquist frequency, and $E[\cdot]$ is the expected value, or average, operator. If $K \gg 1$, $x(n)$ has Gaussian statistics [Rice, 1944, 1945], and thus realizations of a Gaussian process with a specified power spectrum P can be generated using Eq. (1).

3. Simulation of a Quadratically Nonlinear Random Process

The nonrandom phase relationships between triads of Fourier components with frequencies f_1, f_2, and f_1+f_2 of a non-Gaussian random process characterized by quadratic nonlinearities are described statistically by the bispectrum [Hasselmann *et al.*, 1963]. For a discrete-time process, the bispectrum is given by [Haubrich, 1965; Kim & Powers, 1979]

$$B(f_1, f_2) = E[X(f_1)X(f_2)X^*(f_1+f_2)]\,. \qquad (3)$$

If the three Fourier components in the triple product on the right-hand side of Eq. (3) are independent of each other (e.g. if they have random phase relationships such as occur in a Gaussian process), $B(f_1, f_2) = 0$. Owing to symmetry relations, the bispectrum of a discretely sampled, bandlimited process is completely defined by its value in a triangle in (f_1, f_2)-space with vertices at $(0,0)$, $(f_{N/2}, f_{N/2})$, and $(f_N, 0)$ [Hasselmann *et al.*, 1963]. See Nikias and Raghuveer [1987] and Elgar and Chandran [1993] for reviews of properties and applications of bispectra.

Time series that have a nonzero bispectrum cannot be simulated accurately using Eq. (1). However, a quadratically phase coupled time series can be generated by passing a Gaussian process [produced by Eq. (1)] through a quadratic filter (Fig. 1).

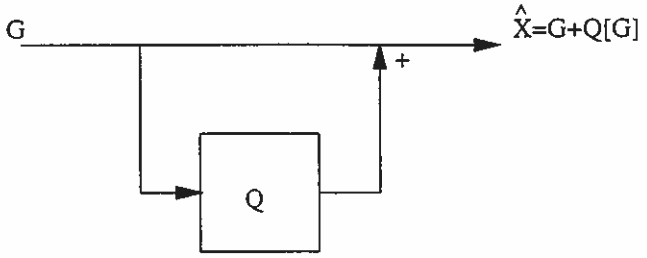

Fig. 1. Block diagram for the filter used to generate a non-Gaussian random process $\hat{X}$ from a Gaussian realization G. The expressions for $\hat{X}$, Q, and $Q[G]$ are given in the text and Appendices.

The Fourier coefficients of the resulting non-Gaussian time series are given by

$$\hat{X}(f_k) = G(f_k) + \sum_{f_l=-f_N}^{f_N} Q(f_l, f_k - f_l)G(f_l) \times G(f_k - f_l),\ -f_N \le f_k \le f_N \qquad (4)$$

where $G(f_k)$ are the Fourier coefficients of the Gaussian time series (with target power spectrum $P(f_k)$) and the quadratic term $Q(f_l, f_k - f_l)$ is the second-order Volterra kernel [Schetzen, 1980].

The power spectrum of a time series generated using Eq. (4) is

$$\hat{P}(f_k) = E[|\hat{X}(f_k)|^2] = P(f_k) + 2\sum_{f_l=-f_N}^{f_N} |Q(f_l, f_k - f_l)|^2 P(f_l) \times P(f_k - f_l),\ -f_N \le f_k \le f_N\,. \qquad (5)$$

By constraining Q to have the same symmetry properties as the bispectrum, the simulated bispectrum Eq. (3) becomes (see Appendix A),

$$\begin{aligned}\hat{B}(f_l, f_m) = {} & 2Q^*(f_l, f_m)[P(f_l)P(f_m) \\ & + P(f_l)P(f_l+f_m) + P(f_m)P(f_l+f_m)] \\ & + 8\sum_{f_a=-f_N}^{f_N} Q(f_a, f_l - f_a)Q(-f_a, f_m + f_a) \\ & \times Q^*(f_l - f_a, f_m + f_a)P(f_a)P(f_l - f_a) \\ & \times P(f_m + f_a),\ -f_N \le f_l, f_m \le f_N\,.\end{aligned} \qquad (6)$$

Because the simulated bispectrum $\hat{B}$ approximates the target bispectrum B, B is substituted for $\hat{B}$ and

Eq. (6) is solved for Q. Assuming the last term in Eq. (6) is small (discussed below), Q becomes

$$Q(f_l, f_m) = \frac{B^*(f_l, f_m)}{2[P(f_l)P(f_m) + P(f_l)P(f_l + f_m) + P(f_m)P(f_l + f_m)]}. \quad (7)$$

Summarizing, to generate a realization of a quadratically nonlinear random process with power spectrum P and bispectrum B, a Gaussian time series (with Fourier coefficients G) is generated using Eq. (1) and then passed through the quadratic filter defined by Eqs. (4) and (7) (Fig. 1). By generating many realizations of the Gaussian process G, a non-Gaussian process with arbitrary degrees of freedom is simulated. If $Q = 0$, a random process with Gaussian statistics is produced.

The power spectrum and bispectrum simulated using the methodology described above are not necessarily identical to their respective target values. Simulated power spectral levels are greater than the target values by an amount equal to the second term on the right hand side of Eq. (5). As shown in Appendix B, for a process with a single phase coupled triad $(f_l, f_m, f_l + f_m)$, the simulated power spectrum at frequency $f_l + f_m$ is too large by an amount that depends on the degree of phase coupling and the amount of power at frequency $f_l + f_m$ relative to the power at f_l and f_m. In the worst case of low power at $f_l + f_m$,

$$\hat{P}(f_l + f_m) = P(f_l + f_m)(1 + b^2(f_l, f_m)) \quad (8)$$

where $b^2(f_l, f_m)$ is the bicoherence squared, given by [Haubrich, 1965; Kim & Powers, 1979],

$$b^2(f_1, f_2) = \frac{|B(f_1, f_2)|^2}{P(f_1)P(f_2)P(f_1 + f_2)}. \quad (9)$$

The bicoherence indicates the relative amount of quadratic phase coupling among the three components of a triad. For no phase coupling, $b(f_1, f_2) = 0$. On the other hand, if all the energy at $f_1 + f_2$ is phase coupled to that at f_1 and f_2, $b(f_1, f_2) = 1$. In the general case of many partially phase coupled triads, the error in the simulated power spectrum is a sum of errors owing to each triad. See Appendix B for details.

Errors in the simulated bispectrum result from neglect of the last term on the right hand side of Eq. (6). In general, the error in $\hat{B}(f_l, f_m)$ has contributions proportional to the sum of products of bicoherences of triads containing at least one of f_l, f_m, or $f_l + f_m$ (Appendix C). For the case of a single phase coupled triad, the error in $\hat{B}$ is zero. For a random process with many strongly phase-coupled triads the error in the simulated bispectrum can be large. See Appendix C for details.

To demonstrate the simulation technique, a target power spectrum consisting of a finite bandwidth primary peak ($f_1 = 0.0625$ Hz in Fig. 2) and its lower energy first ($f_2 = 0.1250$ Hz, Fig. 2) and second ($f_3 = f_1 + f_2 = 0.1875$ Hz, Fig. 2)

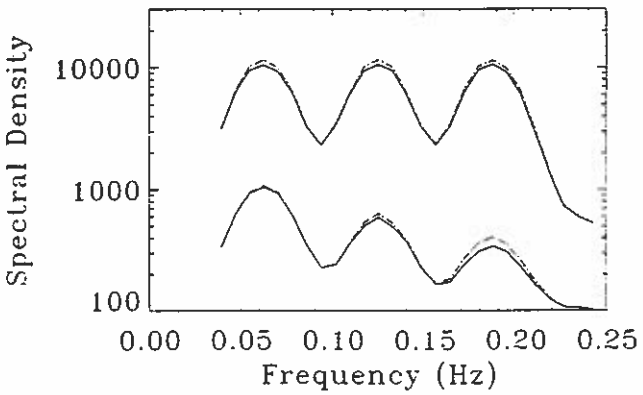

Fig. 2. Power spectra of target (solid curves), simulated time series (dotted curves), and theory [Eq. (5)] (dashed curves) for two different spectral shapes. The simulated and theoretical spectra are nearly indistinguishable. Target bicoherence $b(0.0625, 0.1250) = 0.6$. One set of power spectral values has been offset by a factor of 10 for clarity.

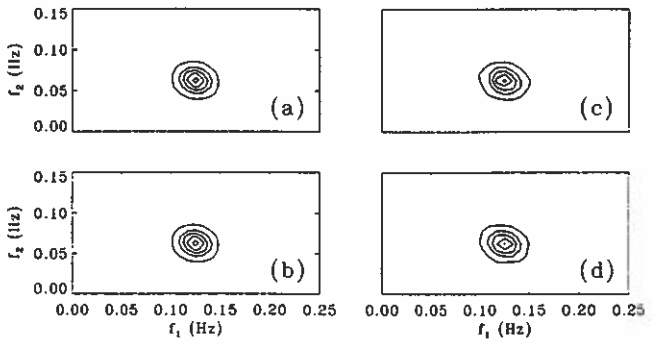

Fig. 3. Contours of real and imaginary parts of the bispectrum. Nonzero values indicate quadratic phase coupling between the Fourier coefficients with frequencies f_1, f_2, and $f_1 + f_2$. (a) real part of the target bispectrum, (b) imaginary part of the target bispectrum, (c) real part of the simulated bispectrum, and (d) imaginary part of the simulated bispectrum. Minimum bispectral contours plotted are $B = 7 \times 10^3$ cm^3/Hz^2, with additional contours every 14×10^3 cm^3/Hz^2. The power spectra are shown in Fig. 2 (decreasing spectral levels in harmonic peaks). Target $b(0.0625, 0.1250) = 0.6$.

harmonics was used. One hundred 16,384-pt Gaussian realizations were generated from the target power spectrum [using Eq. (1)] and passed through the filter shown in Fig. 1 [using Eqs. (4) and (7)] for each of five target bispectra ($0.3 \leq b(f_1, f_2) \leq 0.9$, e.g. Fig. 3). The phase of $B(f_1, f_2) = \pi/4$ in each case. Simulated power spectra and bispectra with the same frequency resolution as the targets were calculated by subdividing each realization into 64 short records and ensemble averaging. The power spectra and bispectra were then averaged over the 100 realizations.

Power spectral levels at the harmonic frequencies for the simulated time series are greater than the target levels, consistent with Eq. (5) and the expected error [Eq. (8), also see Eq. (16) in Appendix B], as shown for $b(f_1, f_2) = 0.6$ in Fig. 2. As discussed in Appendix B, the distribution of error in the simulated power spectrum depends on the spectral shape, and is maximum at the second harmonic ($f_1 + f_2 = 0.1875$ Hz) in this case. For a target spectrum with equal energy in primary and harmonic peaks, there is less relative error in the harmonics and more in the primary, as expected (Fig. 2).

A measure of the fidelity of the overall power spectrum of the simulated time series is the difference between simulated and target second moments (m_2) relative to the target, where the second moment is defined as the mean square of the time series. Consistent with Eqs. (8) and (16), the errors in m_2 increase with increasing bicoherence (Fig. 4). For simulated time series with one phase coupled triad and power spectra shown in Fig. 2, the error in m_2 is less than 15% for $b = 0.9$.

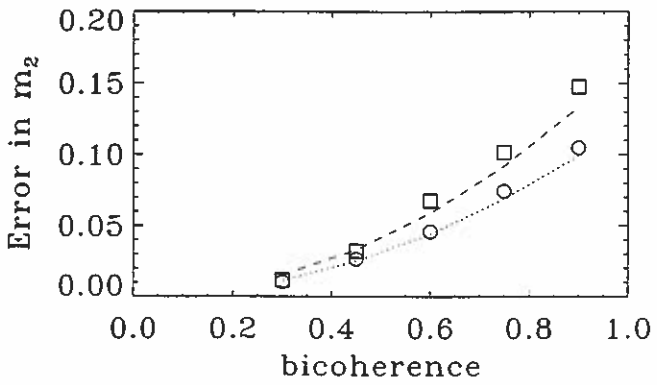

Fig. 4. Error [(simulated-target)/target] in second moment (m_2) of simulated time series versus target bicoherence. Circles are for the spectrum with decreasing energy in the harmonics and squares are for the spectrum with equal energy in primary and harmonic peaks (Fig. 2). The dotted and dashed curves are corresponding theoretical errors in m_2.

The expected error in the bispectrum of a simulated time series is zero if there is only one phase coupled triad (Appendix C), and the small differences between simulated and target bispectra (Fig. 3) are owing to statistical fluctuations in the finite number of realizations (128 degrees of freedom). Similarly there is less than 5% error (not shown) in the real and imaginary parts of the third moments (m_3-real and m_3-imaginary) of the simulated time series, where m_3-real is the mean cube of the time series and m_3-imaginary is the mean cube of the Hilbert transform of the time series. An example of a real time series with a nonzero m_3-imaginary is a sawtooth [Elgar & Guza, 1985].

4. Application to Ocean Surface Gravity Waves

To first order, low amplitude deep water ocean surface gravity waves have Gaussian statistics. Simulations of a Gaussian [e.g. Eq. (1)] sea surface have successfully been used by ocean engineers to investigate probabilities of large waves, average sizes of sequences of waves greater (or less) than a threshold value, and the joint distribution of wave height and period [Goda, 1979; Elgar *et al.*, 1984]. As waves propagate into shallow water (e.g. near the beach) they undergo substantial evolution owing to quadratic nonlinear interactions [Hasselmann *et al.*, 1963; Freilich & Guza, 1984; Elgar & Guza, 1985] resulting in nonzero bispectra and non-Gaussian statistics of the sea surface. Consequently, Gaussian simulations fail to reproduce statistics of waves observed in shallow water [Elgar *et al.*, 1984]. On the other hand, the nonlinear simulation technique developed here can simulate accurately second- and third-order statistics of the sea surface.

The power spectrum and bispectrum of sea-surface elevation observed in 5 m water depth near the beach at Duck, North Carolina are shown in Figs. 5 and 6, respectively. The wave field is dominated by swell ($f = 0.085$ Hz, Fig. 5) arriving from a distant storm. As the waves approach the beach, quadratic nonlinear interactions excite motions with frequency ($f = 0.170$ Hz, Fig. 5) twice that of the swell. This phase coupling (with a maximum $b(0.085, 0.085) = 0.7$) results in nonzero third moments of the sea surface (important for remote sensing [Barrick & Lipa, 1986] and sediment transport [Bowen, 1980]). Realizations of the sea surface

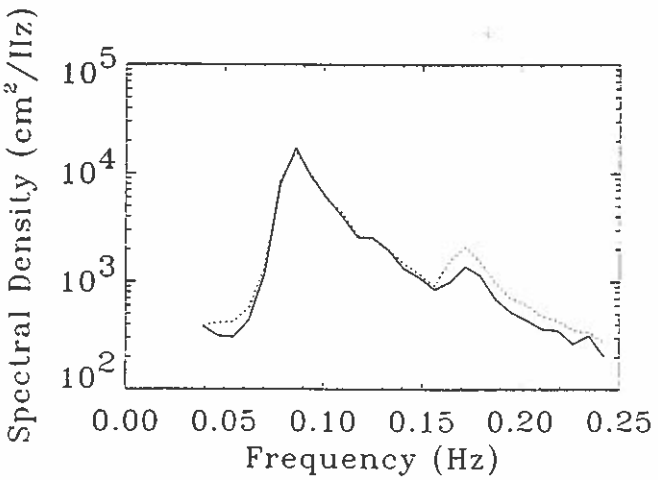

Fig. 5. Power spectra of observed (solid curve) and simulated (dotted curve) sea-surface elevation. The observations (target) were made in 5 m water depth at Duck, North Carolina. There are 128 degrees of freedom.

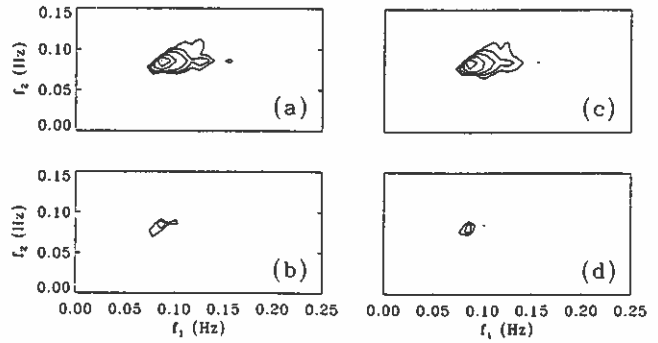

Fig. 6. Contours of real and imaginary parts of the bispectrum of sea-surface elevation. (a) real part of the target (observed) bispectrum, (b) imaginary part of the target bispectrum, (c) real part of the simulated bispectrum, and (d) imaginary part of the simulated bispectrum. Minimum bispectral contours plotted are $B = 1.8 \times 10^5$ cm^3/Hz^2, with additional contours at 3.7×10^5, 7.4×10^5, 1.5×10^6, 3×10^6, and 6×10^6 cm^3/Hz^2. The power spectra are shown in Fig. 5, and the corresponding target $b(0.085, 0.085) = 0.7$.

generated by the nonlinear simulation technique shown in Fig. 1 have power spectrum (Fig. 5) and bispectrum (Fig. 6) similar to the observed (target) values. The simulated power spectrum has more energy at $f = 0.170$ Hz than the observations (Fig. 5), consistent with Eqs. (8) and (16), but simulated third moments (m_3-real $= 6216$ cm^3, m_3-imaginary $= -3$ cm^3) are close to the observed values (m_3-real $= 5826$ cm^3, m_3-imaginary $= 60$ cm^3). This large value of m_3-real corresponds to a wave field dominated by positively skewed waves with narrow crests and wide troughs, whereas the small value of m_3-imaginary indicates that the waves are not pitched forward [Elgar & Guza, 1985; Elgar, 1987]. Additional comparisons between observed and simulated shallow water sea-surface statistics for a wide range of conditions are presented in Vanhoff *et al.* [1997].

5. Conclusions

A technique to generate realizations of quadratically nonlinear time series with specified (target) power spectrum and bispectrum was developed. Gaussian time series, generated using amplitude information from the target power spectrum and random phases are passed through a quadratic filter to introduce quadratic phase coupling. The filter is a function of the target power spectrum and bispectrum. The resulting non-Gaussian time series have power spectra and bispectra similar to target values, with deviations consistent with theory.

Acknowledgments

The research was supported by the Office of Naval Research (Coastal Dynamics and AASERT graduate student support). The observations of ocean waves were obtained in collaboration with R. T. Guza, T. H. C. Herbers, E. Gallagher, and B. Raubenheimer.

References

Alshebeili, S. & Cetin, A. E. [1990] "A phase reconstruction algorithm from bispectrum," *IEEE Transactions on Geoscience and Remote Sensing* **28**(2), 166–170.

Barrick, D. & Lipa, B. [1986] "The second-order shallow-water hydrodynamic coupling coefficient in interpretation of HF radar sea echo," *IEEE J. Oceanic Engineering* **11**, 310–315.

Bondon, P., Benidir, M. & Picinbono, B. [1993] "Polyspectrum modeling using linear or quadratic filters," *IEEE Transactions on Signal Processing* **41**(2), 692–702.

Bondon, P. & Krob, M. [1995] "Blind identifiability of a quadratic stochastic system," *IEEE Trans. Inf. Theory* **41**(1), 245–254.

Bowen, A. J. [1980] "Simple models of nearshore sedimentation; beach profiles and longshore bars," *The Coastline of Canada, Geological Survey of Canada*, 21–30.

Dianat, S. A. & Raghuveer, M. R. [1990] "Fast algorithms for phase and magnitude reconstruction from bispectra," *Optical Engineering* **29**(5), 504–512.

Elgar, S., Guza, R. T. & Seymour, R. J. [1984] "Groups of waves in shallow water," *J. Geophys. Res.* **89**(c3), 3623–3634.

Elgar, S. & Guza, R. T. [1985] "Observations of bispectra of shoaling surface gravity waves," *J. Fluid Mech.* **161**, 425–448.

Elgar, S. [1987] "Relationships involving third moments and bispectra of a harmonic process," *IEEE Transactions on Acoustics, Speech and Signal Processing* **35**(12), 1725–1726.

Elgar, S. & Chandran, V. [1993] "Higher-order spectral analysis to detect nonlinear interactions in measured time series and an application to Chua's circuit," *Int. J. Bifurcations and Chaos* **3**(1), 19–34.

Freilich, M. H. & Guza, R. T. [1984] "Nonlinear effects on shoaling surface gravity waves," *Phil. Trans. R. Soc. Lond.* **A311**, 1–41.

Goda, Y. [1979] "A review of statistical interpretation of wave data," *Port and Harbor Res. Inst.* **18**, 5–32.

Hasselmann, K., Munk, W. & MacDonald, G. [1963] "Bispectra of ocean waves," ed. Rosenblatt, M., *Time Series Analysis*, pp. 125–139, Wiley.

Haubrich, R. A. [1965] "Earth noise, 5 to 500 millicycles per second," *J. Geophys. Res.* **70**(6), 1415–1427.

Kim, Y. C. & Powers, E. J. [1979] "Digital bispectral analysis and its applications to nonlinear wave interactions," *IEEE Trans. Plasma Sci.* PS-7(2), 120–131.

Matsuoka, T. & Ulrych, T. J. [1984] "Phase estimation using the bispectrum," *Proc. IEEE* **72**(10), 1403–1411.

Nikias, C. L. & Raghuveer, M. R. [1987] "Bispectrum estimation: A digital signal processing framework," *Proc. IEEE* **75**(7), 869–891.

Rice, S. O. [1944] "The mathematical analysis of random noise," *Bell Syst. Tech. J.* **23**, 282–332.

Rice, S. O. [1945] "The mathematical analysis of random noise," *Bell Syst. Tech. J.* **24**, 46–156.

Schetzen, M. [1980] *The Volterra and Wiener Theories of Nonlinear Systems*, New York, Wiley.

Theiler, J., Eubank, S., Longtin, A., Galdrikian B. & Farmer, J. D. [1992] "Testing for nonlinearity in time series: the method of surrogate data," *Physica* **D58**, 77–94.

Vanhoff, B., Elgar, S. & Guza, R. T. [1997] "Numerically simulating non-Gaussian sea surfaces," *ASCE J. Waterway, Port, Coastal and Ocean Engineering* **123**(2), 68–72.

Appendix A

The simulated bispectrum $\hat{B}_{l,m}$ is calculated by substituting Eq. (4) into Eq. (3), yielding

$$\hat{B}_{l,m} = E\left[\left(G_l + \sum_{f_n=-f_N}^{f_N} Q_{n,l-n} G_n G_{l-n}\right) \times \left(G_m + \sum_{f_o=-f_N}^{f_N} Q_{o,m-o} G_o G_{m-o}\right) \times \left(G_{l+m} + \sum_{f_p=-f_N}^{f_N} Q_{p,l+m-p} G_p G_{l+m-p}\right)^*\right], \quad -f_N \le f_l,\, f_m \le f_N \tag{10}$$

where $\hat{B}_{l,m} = \hat{B}(f_l, f_m)$ is the simulated bispectrum, $G_k = G^*_{-k} = G(f_k)$ are the Fourier coefficients of the Gaussian simulation, $Q_{l,m} = Q(f_l, f_m)$ is the second order Volterra kernel, and $E[\cdot]$ is the expected value (or average) operator. Because odd moments of a Gaussian process are zero, the only terms that will contribute to the expected value in Eq. (10) are the 4th and 6th order (in G) terms that can be written as $Q_{i,j}E[|G_i|^2|G_j|^2]$, $Q_{i,i}E[|G_i|^4]$, or $QQQE[|G_i|^2|G_j|^2|G_k|^2]$ (shown in greater detail below). For 4th order terms (i.e. terms containing $E[G_iG_jG_kG_l]$) either ($f_i = -f_j$, $f_k = -f_l$), ($f_i = -f_k$, $f_j = -f_l$), or ($f_i = -f_l$, $f_j = -f_k$). Thus (for $l \neq m$)

$$\begin{aligned} B^4_{l,m} = E[&G_lG_m(Q^*_{l,m} + Q^*_{m,l})G^*_lG^*_m \\ &+ G_l(Q_{-l,l+m} + Q_{l+m,-l})G_{-l}G_{l+m}G^*_{l+m} \\ &+ (Q_{-m,l+m} + Q_{l+m,-m})G_{-m}G_{l+m}G_mG^*_{l+m}] \end{aligned} \tag{11}$$

where $B^4_{l,m}$ is the part of the simulated bispectrum containing terms that are 4th order in G. Because Q has the same symmetry properties as the bispectrum (i.e. $Q_{l,m} = Q_{m,l} = Q^*_{-l,l+m} = Q^*_{-m,l+m}$), substituting $E[|G_l|^2|G_m|^2] = P_lP_m$, where $P_l = P(f_l)$ (i.e. the target power spectrum), yields

$$B^4_{l,m} = 2Q^*_{l,m}(P_lP_m + P_lP_{l+m} + P_mP_{l+m}). \tag{12}$$

For $l = m$, the first term in Eq. (11) does not contain both $Q^*_{l,m}$ and $Q^*_{m,l}$ but only a single $Q^*_{l,l}$. However, Eq. (12) still holds because $E[|G_l|^4] = 2P_l^2$.

Similarly, terms containing $E[G_iG_jG_kG_lG_m G_n]$, (i.e. 6th order terms) must have either ($f_i = -f_j$, $f_k = -f_l$, $f_m = -f_n$), ($f_i = -f_j$, $f_k = -f_m$, $f_l = -f_n$), or ($f_i = -f_j$, $f_k = -f_n$, $f_l = -f_m$) (or one of 12 other similar combinations) to contribute to the expected value in Eq. (10). Thus

$$\begin{aligned} B^6_{l,m} = E\Bigg[&\sum_{f_a=-f_N}^{f_N} (Q_{a,l-a} + Q_{l-a,a})G_aG_{l-a} \\ &\times (Q_{-a,m+a} + Q_{m+a,-a})G_{-a}G_{m+a} \\ &\times (Q^*_{l-a,m+a} + Q^*_{m+a,l-a})G^*_{l-a}G^*_{m+a}\Bigg] \end{aligned}$$

$$= 8 \sum_{f_a=-f_N}^{f_N} Q_{a,l-a} Q_{-a,m+a} Q^*_{l-a,m+a} \times P_a P_{l-a} P_{m+a},\ -f_N \le f_l,\ f_m \le f_N \qquad (13)$$

where $B^6_{l,m}$ is the part of the simulated bispectrum containing terms that are 6th order in G. Because $\hat{B}_{l,m} = B^4_{l,m} + B^6_{l,m}$, Eq. (6) follows. The processes to be simulated have zero mean, thus all triads containing a DC component have zero bispectrum, and $Q_{0,i} = Q_{i,0} = Q_{-i,i} = 0$.

Appendix B

For a process with one phase coupled triad (f_l, f_m, $f_l + f_m$), the simulated power spectrum at frequency $f_l + f_m$ [Eq. (5)] becomes

$$\hat{P}_{l+m} = P_{l+m} + 2(|Q_{l,m}|^2 P_l P_m + |Q_{m,l}|^2 P_m P_l) \qquad (14)$$

where P_{l+m} is the target power spectral value at $f_l + f_m$ and $Q_{l,m}$ is the second order Volterra kernel. The bispectrum can be rewritten as [using Eq. (9)]

$$B_{l,m} = b_{l,m} e^{j\beta_{l,m}} \sqrt{P_l P_m P_{l+m}} \qquad (15)$$

where $b_{l,m} = b(f_l, f_m)$ is the bicoherence and $\beta_{l,m}$ is the phase of $B_{l,m}$. Thus, using Eqs. (7) and (15), the simulated power spectrum [Eq. (14)] becomes

$$\hat{P}_{l+m} = P_{l+m} + \frac{b^2_{l,m} P_l^2 P_m^2 P_{l+m}}{(P_l P_m + P_l P_{l+m} + P_m P_{l+m})^2} = P_{l+m}(1 + |\alpha_{l,m}|^2) \qquad (16)$$

where

$$\alpha_{l,m} = \frac{b_{l,m} e^{-j\beta_{l,m}}}{(1 + P_{l+m}/P_m + P_{l+m}/P_l)} \qquad (17)$$

and $|\alpha_{l,m}| < b_{l,m} \le 1$. If $P_{l+m} \gg P_l$, P_m, the error in P_{l+m} is small. However, if $P_{l+m} \ll P_l, P_m$

$$\hat{P}_{l+m} \to P_{l+m}(1 + b^2_{l,m}). \qquad (18)$$

Similar expressions can be written for $\hat{P}_l$ and $\hat{P}_m$. The error in the simulated power spectrum is thus distributed among all three frequencies in the triad (i.e. f_l, f_m, and $f_l + f_m$) in proportion to $\alpha_{-m,l+m}$, $\alpha_{-l,l+m}$, and $\alpha_{l,m}$, respectively.

Appendix C

The last term in Eq. (6) (i.e. the theoretical error in the simulated bispectrum) is equal to

$$B^6_{l,m} = 8 \sum_{f_a=-f_N}^{f_N} Q_{a,l-a} Q_{-a,m+a} Q^*_{l-a,m+a} \times P_a P_{l-a} P_{m+a},\ -f_N \le f_l,\ f_m \le f_N \qquad (19)$$

where $B^6_{l,m}$ is the 6th order term in the simulated bispectrum (Appendix A), $Q_{l,m}$ is the second order Volterra kernel, and P_k is the target power spectrum at frequency f_k. Substituting Eqs. (7) and (15) into Eq. (19) yields

$$\begin{aligned} B^6_{l,m} &= \sqrt{P_l P_m P_{l+m}} \sum_{f_a=-f_N}^{f_N} \frac{b_{a,l-a} e^{-j\beta_{a,l-a}}}{(1 + P_l/P_{l-a} + P_l/P_a)} \\ &\quad \times \frac{b_{-a,m+a} e^{-j\beta_{-a,m+a}}}{(1 + P_m/P_{m+a} + P_m/P_{-a})} \\ &\quad \times \frac{b_{l-a,m+a} e^{+j\beta_{l-a,m+a}}}{(1 + P_{l+m}/P_{m+a} + P_{l+m}/P_{l-a})} \\ &= \sqrt{P_l P_m P_{l+m}} \sum_{f_a=-f_N}^{f_N} \alpha_{a,l-a} \alpha_{-a,m+a} \alpha^*_{l-a,m+a}, \\ &\quad -f_N \le f_l,\ f_m \le f_N \end{aligned} \qquad (20)$$

where $\alpha_{l,m}$ is given by Eq. (17). Thus, the simulated bispectrum can be written as the sum of 4th and 6th order terms (Appendix A),

$$\begin{aligned} \hat{B}_{l,m} &= B^4_{l,m} + \sum_{f_a=-f_N}^{f_N} \alpha_{a,l-a} \alpha_{-a,m+a} \alpha^*_{l-a,m+a} \times \sqrt{P_l P_m P_{l+m}} \\ &= B_{l,m} + \sum_{f_a=-f_N}^{f_N} \alpha_{a,l-a} \alpha_{-a,m+a} \alpha^*_{l-a,m+a} \times \sqrt{P_l P_m P_{l+m}},\ -f_N \le f_l,\ f_m \le f_N . \end{aligned} \qquad (21)$$

For processes with a single phase coupled triad (f_l, f_m, $f_l + f_m$), there are only six nonzero α's ($\alpha_{l,m}$, $\alpha_{m,l}$, $\alpha_{-l,l+m}$, $\alpha_{l+m,-l}$, $\alpha_{-m,l+m}$, and $\alpha_{l+m,-m}$). Thus, for the triple product on the right hand side of Eq. (21) to be nonzero, f_a must equal $\pm f_l$, $\pm f_m$, or $\pm(f_l + f_m)$. For $f_a = f_l$ the product becomes $\alpha_{l,0} \alpha_{-l,m+l} \alpha^*_{0,m+l} = 0$ (because the processes that

are being simulated have zero mean, implying $b_{i,0} = b_{0,i} = 0$, and thus $\alpha_{l,0} = \alpha_{l,0} = 0$). For $f_a = f_m$, $\alpha_{m,l-m}\alpha_{-m,2m}\alpha^*_{l-m,2m} = 0$ (because $\alpha_{m,l-m} = \alpha_{-m,2m} = \alpha^*_{l-m,2m} = 0$), and for $f_a = f_l + f_m$, $\alpha_{l+m,-m}\alpha_{-l-m,l+2m}\alpha^*_{-m,l+2m} = 0$ (because $\alpha_{-l-m,l+2m} = \alpha^*_{-m,l+2m} = 0$). The same can be shown for $f_a = -f_l$, $f_a = -f_m$, and $f_a = -f_l - f_m$. Thus, for processes with a single phase coupled triad, the error in the simulated bispectrum is zero.